General Material Models for Electromagnetic Field-Tissue Interaction

T. M. Benson[1], C. Christopoulos, D. W. P. Thomas, J. Paul,
S. Greedy, P. Sewell, D. McKirdy and A. Vukovic

***Abstract*— There has been significant interest in recent years on the interaction of electromagnetic fields with biological tissues for health, diagnostic and therapeutic reasons and also the optimum design of antennas in close proximity to the body such as those found in mobile phones. It is therefore necessary to devise suitable broadband models of the dielectric properties of biological materials which may be used in time domain simulations for analysis and design purposes. This paper details model parameter values for biological tissues and shows typical simulation results for a human head in the vicinity of a radiating half-wave dipole.**

***Index Terms*— Time-domain electromagnetics, Frequency-dependent dielectric materials, Transmission-line modelling.**

I. Introduction

The requirement for the accurate analysis of the interaction between electromagnetic fields and human tissues has become an integral part of the design process. The increased demand to meet specific absorption rate (SAR) limitations in the communications industry as well as optimizing antenna design, together with the requirements of medical applications, has increased the need for accurate broadband models describing material behaviour in the presence of electromagnetic fields.

In frequency-domain electromagnetic simulations, the lossy nature of the dielectric properties of biological tissues is easily described by using a complex relative permittivity. For simulations at different frequencies, the numerical values of this complex relative permittivity must be adjusted because it is a strong function of frequency in the case of biological tissues. In a simple electromagnetic simulation, the complex relative permittivity $\varepsilon_r^\star$ is modelled using a constant real part ε_r' to give energy storage and a constant conductivity term σ_e to give energy loss, i.e.,

$$\varepsilon_r^\star(\omega) = \varepsilon_r'(\omega) - j\varepsilon_r''(\omega) = \varepsilon_r' - j\left(\frac{\sigma_e}{\omega\varepsilon_0}\right) \tag{1}$$

In (1), ε_r'' is the imaginary relative permittivity, ω is the angular frequency and ε_0 is the permittivity of free-space. Although (1) gives a variation of ε_r'' with frequency, ε_r' is fixed. Since from the Kramers-Krönig relation, e.g. [1], the real and imaginary parts of the relative permittivity are conjugate functions, having the real part fixed and the imaginary part varying is non-physical. Thus for the simulation of the measured relative permittivity of biological tissues, e.g. [2], [3] over a wide bandwidth, it is necessary to use a more sophisticated function than (1). The functions used here to implement the models are described in section II. In section III, the results obtained using these functions in the study of half-wave dipole antennas near to a human head are shown. Simulations of this type are useful in quantifying the interaction of mobile phones with the human head.

[1]All authors are with the George Green Institute for Electromagnetics Research, School of Electrical and Electronic Engineering, University of Nottingham, Nottingham, NG7 2RD, United Kingdom. Email: trevor.benson@nottingham.ac.uk

This paper was presented at TELSIKS 2005 Conference, Serbia and Montenegro

II. Formulation

As detailed in [2], [3], the frequency dependence of the relative permittivity $\varepsilon_r^\star(s)$ of many biological tissues can, over a wide frequency range, be accurately described using the function

$$\varepsilon_r^\star(s) = \varepsilon_{r\infty}^c + \sum_{i=0}^{NP^c-1} \frac{\Delta\chi_{ei}^c}{1+(s\tau_{ei}^c)^{1-\alpha_i}} \tag{2}$$

In (2), $\varepsilon_{r\infty}^c$ is the relative permittivity at high frequencies, s is the Laplace variable and NP^c is the number of poles. For the ith pole, $\Delta\chi_{ei}^c$ is the electric susceptibility contrast, τ_{ei}^c is the relaxation time and α_i is the Cole-Cole parameter, where $0 \leq \alpha_i \leq 1$ [4]. The superscript c denotes a Cole-Cole coefficient. The parameters required in (2) are tabulated in reference [3] for various types of human tissue.

Although using Cole-Cole parameters α_i adds extra flexibility to the frequency-domain parameterization of dielectric response, the time-domain transform of (2) cannot be solved recursively. A systematic approach for obtaining a recursive solution of (2) is to apply the frequency-domain Prony method [5], [6] to a set of complex data obtained from the evaluation of (2) over the frequency range of interest. This leads to a multiple Debye approximation [7]

$$\varepsilon_r^\star(s) = \varepsilon_{r\infty} + \sum_{i=0}^{NP-1} \frac{\Delta\chi_{ei}}{1+s\,\tau_{ei}} \tag{3}$$

Note the coefficients in (2) and (3) do not have the same numerical values and the number of poles may be different. In general, more poles are required in the multiple Debye description compared with the Cole-Cole description. The time-domain transform of (3) can be solved recursively using standard $\mathcal{Z}$-transform techniques [8]. Over the frequency range 10MHz–20GHz, an adequate approximation to the tissue properties was obtained using four Debye poles, i.e.

$$\varepsilon_r^\star(s) = \varepsilon_{r\infty} + \sum_{i=0}^{3} \frac{\Delta\chi_{ei}}{1+s\,\tau_{ei}} \tag{4}$$

TABLE I

PARAMETERS FOR THE FOUR POLE DEBYE MODELS OF BIOLOGICAL TISSUES OCCURRING IN THE HUMAN HEAD VALID OVER THE FREQUENCY RANGE 10MHz–20GHz

tissue type	$\varepsilon_{r\infty}$	$\Delta\chi_{e0}$	τ_{e0} (psec)	$\Delta\chi_{e1}$	τ_{e1} (psec)	$\Delta\chi_{e2}$	τ_{e2} (psec)	$\Delta\chi_{e3}$	τ_{e3} (nsec)
blood	6.30755	32.1491	6.13337	19.8835	14.6686	12.0503	235.489	16289.4	123.394
bone (cortical)	3.07575	3.41899	5.88266	4.68891	18.4689	2.62162	133.307	263.844	41.4808
brain (grey matter)	6.06879	28.0078	6.09317	14.5362	15.3029	20.5258	297.450	1408.66	27.1203
brain (white matter)	5.50610	20.0020	6.08969	10.4210	15.3627	13.6421	279.577	773.540	26.5769
cerebellum	5.92455	25.6507	6.18446	12.7113	16.0373	30.2458	343.807	1702.04	23.3245
cerebrospinal fluid	6.72819	38.0571	5.92124	21.8579	14.1223	13.0558	299.597	159050	690.219
cornea	6.16873	29.5233	6.05542	15.6706	15.0457	16.7983	264.141	10900.8	100.782
dura	6.62308	21.7636	5.53870	13.6131	15.7324	13.6648	301.728	5339.36	73.6750
eye tissues (sclera)	6.15572	29.8314	5.97052	16.6493	14.4530	9.98595	125.120	12060.0	125.120
fat (average infiltrated)	3.26263	4.37566	5.04492	3.08728	15.9096	1.36669	138.073	472.198	67.8070
fat (not infiltrated)	2.75747	1.47201	5.09112	1.02432	16.1687	0.562393	166.071	307.072	82.0218
lens cortex	5.78725	24.8212	5.94389	14.0890	14.2826	6.65587	209.517	6404.06	100.456
lens nucleus	5.26603	17.5873	6.29511	12.1895	14.9174	7.26757	235.941	2121.56	71.3974
muscle	6.33105	31.7247	5.66503	14.6529	14.0634	8.75244	223.629	9282.15	124.022
nerve	5.20575	16.2527	6.09887	8.43983	15.4000	11.5931	272.432	1408.15	43.3356
skin (dry)	4.11627	32.4311	7.23103	1.59917	36.1674	24.7148	446.831	766.294	16.8827
skin (wet)	5.77139	24.1188	6.07266	12.6871	15.1717	15.5647	271.566	2530.09	49.4856
tendon	5.19809	15.6020	7.04120	22.8103	16.4840	6.67945	173.033	6590.35	129.913
thyroid	6.32455	32.2984	5.92012	18.6409	14.1753	7.51191	163.588	13988.3	163.588
tongue	6.15235	29.7954	5.96608	16.6810	14.4320	9.78596	222.013	6335.36	89.7499
trachea	4.16610	22.8939	5.99444	12.6007	14.6306	8.88381	230.434	5829.20	102.185
vitreous humor	3.99908	65.0032	7.23404					4.80×10^6	28263.0

The parameters required in (4) for simulation of the 22 types of biological tissues occurring in the human head calculated using the data from reference [3] are given in Table I.

As described in [3], the Cole-Cole functions used as the starting point of this work were developed from a comprehensive survey of the literature and these models represent the best fit possible using a limited number of Debye dispersions. We have found that our comparisons of the Debye and Cole-Cole models over the frequency range 10MHz–20GHz shows that the deviation between the models is within the spread of experimental data.

The models were used in a three-dimensional time-domain electromagnetic solver based on the Transmission-Line Modelling (TLM) method. The details of the field simulation technique adopted here are described in [9] and the method for incorporation of the multiple Debye dielectric material properties into the approach is described in [8]. Other related work in the Finite-Difference Time-Domain (FDTD) technique includes the $\mathcal{Z}$-transform approach [10] and the differential equation solution [11].

III. RESULTS: HALF-WAVE DIPOLE—HUMAN HEAD INTERACTION

In this section results are shown from four simulations of an anatomically correct human head model based on a 3mm grid. The computational grid consisted of $101\times155\times101$ cells and was iterated for 4444 time-steps. The external boundaries were matched and each simulation took about 3.5 cpu hours on an Itanium^2 ZX6000 workstation and required 542MB of RAM. Two frequencies were considered, i.e. 900MHz and 1800MHz and two antenna polarizations were used, horizontally polarized (HP) and vertically polarized (VP).

A. 900MHz HP

In the first simulation, a HP half-wave dipole excited with a voltage source at 900MHz having a peak value of 12V was placed 9mm from the head with its centre close to the left hand ear canal. The dipole consisted of 55 cells and was simulated using short-circuit boundary conditions on the cells describing the dipole. The power output of the dipole was 0.5W. The maximum electric fields observed for an axial cut, coincident with the centre of the dipole, over the last source cycle were logged and are shown in Fig. 1. In this figure, the dipole position, the outline of the head and detail of the internal structure of the head are clearly visible.

B. 900MHz VP

The second simulation was similar to the first except the dipole was VP. The maximum electric fields obtained for the same axial cut as in Fig. 1 are shown in Fig. 2. This figure does not show as much detail inside the head, although the outline of the head may still be discerned. However a standing wave pattern inside the head can clearly be seen.

C. 1800MHz HP

In the third simulation, a horizontally polarized half-wave dipole excited with a voltage source at 1800MHz having a peak value of 12V was placed 9mm from the head with the gap close to the left hand ear canal. The dipole consisted of 27 cells and the power output was 0.45W. The maximum electric fields observed for an axial cut over the last source cycle were logged and are shown in Fig. 3. Similar to Fig. 1, the internal details of the head are clearly visible and also a guiding effect through the ear canals and nasal cavities is apparent leading to a radiation lobe on the opposite side of the head to where the dipole is placed.

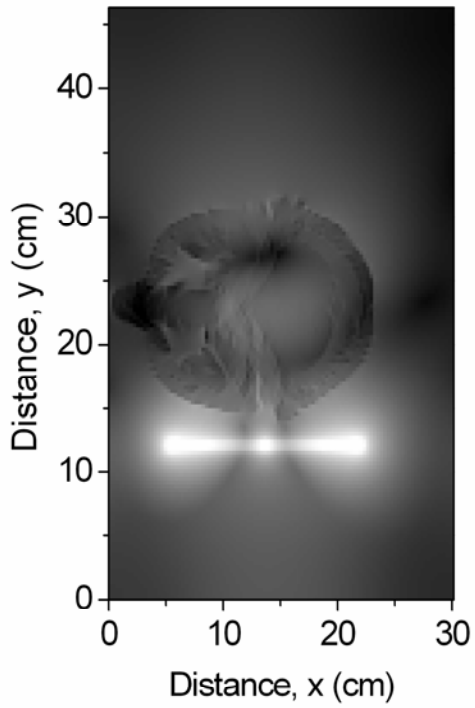

Fig. 1. The maximum electric fields in and around the head for interaction with a 900MHz horizontally polarized half-wave dipole

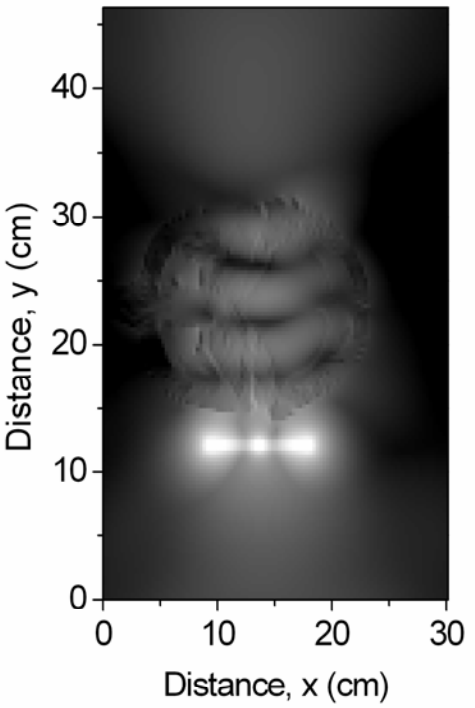

Fig. 3. The maximum electric fields in and around the head for an 1800MHz horizontally polarized half-wave dipole

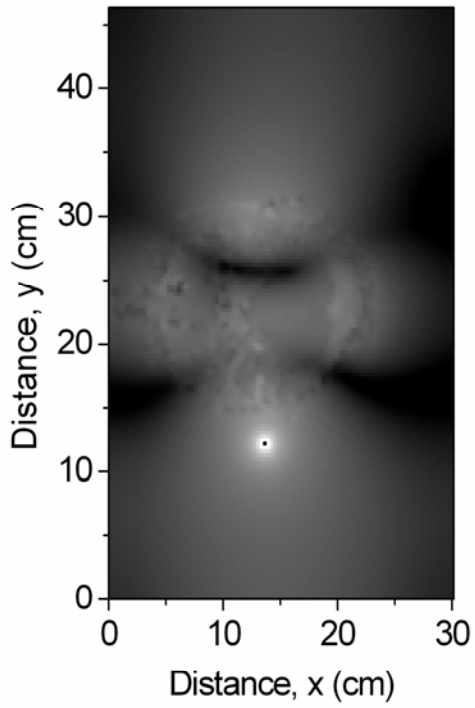

Fig. 2. The maximum electric fields in and around the head for a 900MHz vertically polarized half-wave dipole

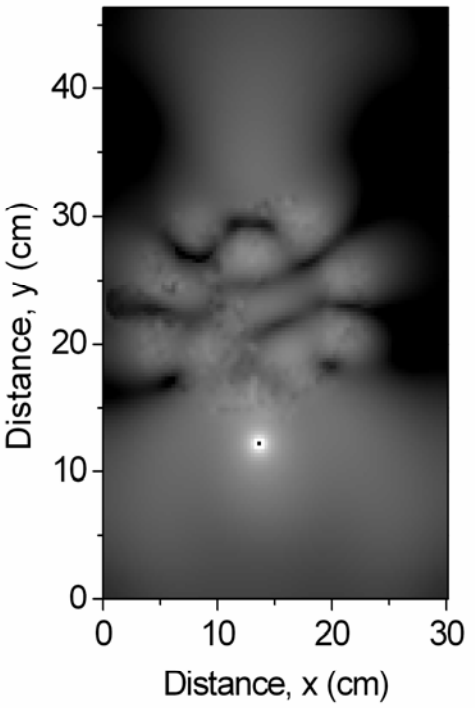

Fig. 4. The maximum electric fields in and around the head for an 1800MHz vertically polarized half-wave dipole

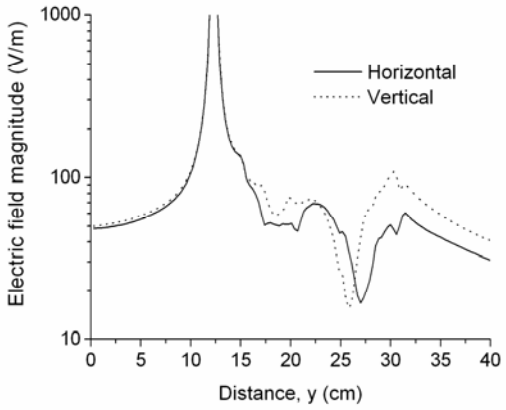

Fig. 5. Maximum electric field observed along a y-directed line through the antenna gap for horizontally and vertically polarized 900MHz half-wave dipoles

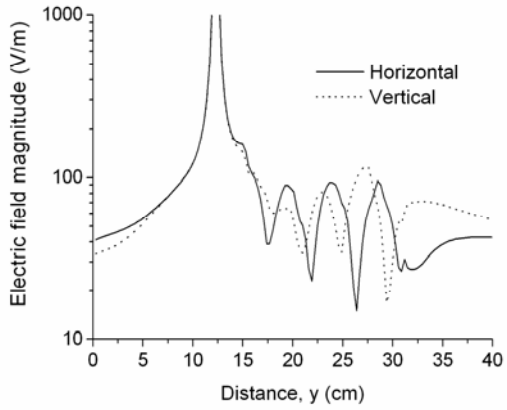

Fig. 6. Maximum electric field observed along a y-directed line through the antenna gap for horizontally and vertically polarized 1800MHz half-wave dipoles

D. 1800MHz VP

The final simulation was similar to the previous one except the dipole was VP. The maximum electric fields obtained for an axial cut are in Fig. 4. Similar to Fig. 2, the internal details of the head are not visible. The radiation pattern is complex with six observable lobes.

E. Comparison of results

In Fig. 5 the maximum electric fields observed along a y-directed line through the antenna gap for HP and VP half-wave dipoles at 900MHz is shown. Similarly, Fig. 6 shows the maximum electric fields observed along a y-directed line through the antenna gap for HP and VP half-wave dipoles at 1800MHz. In these figures, the standing-wave patterns in the head are evident: just one standing wave null is produced at 900MHz and three are produced at 1800MHz. The peak electric fields inside the head in these cases is of the order of $|E_{pk}| \sim 100$V/m so for tissue having an effective conductivity of $\sigma_e^{eff} \sim 1$S/m and a typical mass density of $\rho \sim 1050$kg/m^3, the SAR is of the order of

$$\mathrm{SAR} = \frac{\sigma_e^{eff}|E_{pk}|^2}{2\rho} \sim 5\mathrm{W/kg} \qquad (5)$$

Note this calculation gives the SAR at a point, whereas the European and US regulations pertaining to power deposition in human tissue are defined using the point SAR averaged over 1g or 10g of tissue.

IV. Conclusion

In this paper we have outlined an approach for the time-domain simulation of the electromagnetic fields induced in a biological tissues. Details of the multiple Debye approximation were described and parameters for 22 types of biological tissues were given. The examples considered here involved a human head in the proximity of a half-wave radiating dipole. The fields in and around the head were shown for the standard mobile telephone frequencies of 900MHz and 1800MHz for horizontally and vertically polarized antennas.

References

[1] J. A. Kong. *Electromagnetic Wave Theory*. Wiley, New York, 1986.

[2] S. Gabriel, R. W. Lau and C. Gabriel. The dielectric properties of biological materials: III. Parametric models for the dielectric spectrum of tissues. *Phys. Med. Biol.*, 41:2271–2293, 1996.

[3] C. Gabriel, and S. Gabriel. Compilation of the Dielectric Properties of Body Tissues at RF and Microwave Frequencies. Technical Report AFOSR/NL Bolling AFB DC 20332-0001, Physics Department, King's College London, London, WC2R 2LS, UK, June 1996.

[4] K. S. Cole and R. H. Cole. Dispersion and Absorption in Dielectrics—I.Alternating Current Characteristics. *Journal of Chemical Physics*, 9:341–351, April 1941.

[5] J. N. Brittingham, E. K. Miller and J. L. Willows. Pole Extraction from Real-Frequency Information. *Proceedings of the IEEE*, 68(2):263–273, February 1980.

[6] J. Paul, V. Podlozny and C. Christopoulos. The Use of Digital Filtering Techniques for the Simulation of Fine Features in EMC Problems Solved in the Time-Domain. *IEEE Transactions on Electromagnetic Compatibility*, 45(2):238–244, May 2003.

[7] W. D. Hurt. Multiterm Debye Dispersion Relations for Permittivity of Muscle. *IEEE Transactions on Biomedical Engineering*, 32(1):60–64, January 1985.

[8] J. Paul, C. Christopoulos and D. W. P. Thomas. Simulation of general linear dielectric properties in TLM. *International Journal of Numerical Modelling*, 15(5):403–417, September 2002.

[9] J. Paul, C. Christopoulos and D. W. P. Thomas. Generalized Material Models in TLM—Part 1: Materials with Frequency-Dependent Properties. *IEEE Transactions on Antennas and Propagation*, 47(10):1528–1534, October 1999.

[10] D. M. Sullivan. Frequency Dependent FDTD Methods using Z-transform. *IEEE Transactions on Antennas and Propagation*, 40(10):1223–1230, October 1992.

[11] O. P. Gandhi, B. Q. Gao and J. Y. Chen. A Frequency-Dependent Finite-Difference Time-Domain Formulation for General Dispersive Media. *IEEE Microwave and Guided Wave Letters*, 41(4):658–665, April 1993.